JOURNAL OF CATALYSIS 153, 17–24 (1995)

Preparation of High Surface Area Mo/ZrO_2 Catalysts by a Molten Salt Method: Application to Hydrodesulfurization

Pavel Afanasiev, Christophe Geantet, and Michèle Breysse

Institut de Recherches sur la Catalyse, 2 Avenue Albert Einstein, 69626 Villeurbanne Cedex, France

Received May 16, 1994; revised November 18, 1994

Supported molybdenum oxide on zirconia catalysts were prepared by simultaneous reaction of Zr oxychloride and ammonium heptamolybdate in molten K–Na nitrate eutectic at 773 K. It was shown that Zr(IV) and Mo(VI) salts react in the molten nitrate medium leading to solids of high specific surface areas (up to 200 m^2/g). The solids consist of small crystallites of tetragonal ZrO_2 containing polymolybdate species on their surface. Textural properties of the catalysts and their stability to calcination in air were studied as a function of the initial Mo/Zr ratio in the reaction mixture. Surface polymolybdate species stabilize tetragonal zirconia and improve the textural properties of the system. Surface areas twice those obtained by conventional methods were observed. Catalytic activity of samples was studied by the thiophene hydrodesulfurization reaction. Due to the enhanced surface area, Mo loading could be increased up to 12.5 wt% of Mo without loss of intrinsic activity per Mo atom. © 1995 Academic Press, Inc.

INTRODUCTION

Supported molybdenum oxide catalysts are extremely important for industrial applications. These systems are active for various reactions, such as partial oxidation of hydrocarbons (1–3), metathesis of alkenes (4), and hydrotreatment (5–7). Different procedures may be used for depositing the active compound on the support. The conventional way is to impregnate the high surface area support oxide with an aqueous solution of ammonium heptamolybdate at a given pH followed by calcining the solid in air. Usually the supports are alumina or silica, but considerable interest is now devoted to other supports such as oxides of titanium (8), niobium (9), and zirconium (10–12). The latter oxide provides original surface properties and its interactions with the deposited molybdenum are favorable for applications in hydrotreatment (13). The extreme hardness and high specific mass of zirconia can also be an advantage. Several authors have shown the hydrotreating properties of Mo/ZrO_2 catalysts to be better than those of classical systems (14–17). The specific activity of Mo at low surface concentration on zirconia was found to be significantly higher than that for alumina or silica. Therefore, if a sufficient amount of Mo could be dispersed at low surface coverage on zirconia, then a more active catalyst would result. However, there are difficulties in obtaining titania or zirconia with a thermally stable high surface area. In fact, the preparation conditions can strongly influence the textural properties of ZrO_2 (18, 19). Usually, zirconia supports are prepared by precipitation from aqueous solution (20). After calcination in air at 673–873 K, the surface areas of the oxide do not exceed 100 m^2/g and rapid sintering occurs at elevated temperatures. It is possible to stabilize and slightly enhance the surface area of this support by incorporating foreign elements such as yttrium, nickel, or aluminum (21). However, although improved, the textural properties of such catalysts are still considerably below those of catalysts based on industrial alumina supports.

Recently, it was demonstrated that the use of nitrate melts as reaction media produced highly divided oxide particles at a relatively low temperature. The molten salt method was applied for preparing ceramic precursors (22) or catalytic supports (15, 23) of pure or yttria-stabilized zirconia. These solids had surface areas as high as 130 m^2/g and pore radii in the range 20–80 Å. Dispersion and sulfidation of molybdenum on this support provided intrinsic activities (Mo loading of 2.8 atom/nm^2) in the thiophene HDS model reaction twice those of conventional alumina (23). Furthermore, NiMo catalysts were also found to exhibit promising activities for hydrogenation and hydrodenitrogenation reactions (15). These results initiated further work on the properties of molten nitrates as a medium for solid synthesis. The present paper deals with the development of a one-step synthesis of the MoO_3/ZrO_2 system in the molten nitrate. Characterization of the solid products, their sulfidation, and their applications to a model hydrotreating reaction (HDS of thiophene) are presented here. Detailed studies on the mechanism of molten salt synthesis and on the role of molybdenum in thermal stability were carried out and will be published elsewhere (24, 25).

0021-9517/95 $6.00

EXPERIMENTAL

Preparation of Catalysts

Ammonium heptamolybdate tetrahydrate was mixed with zirconium oxychloride octahydrate and a 10-fold molar excess of Na–K nitrate eutectic (45 wt% $NaNO_3$–55 wt% KNO_3). The Mo/Zr atomic ratio varied in the range 0.01–0.4. Reaction mixtures were pretreated under a flow of dry nitrogen for 2 h, at 423 K, in order to eliminate water from hydrated salts, before the temperature was increased to 773 K, and held at this temperature for 2 h to carry out the reaction. The reaction mixture was cooled to room temperature and the solidified melt extracted, being then thoroughly washed by distilled water to remove all the soluble salts from the oxide product. The samples were dried overnight at 393 K in air. Calcination of the samples was carried out at 873 or 1073 K under a flow of dry air for 2 h.

HDS of Thiophene

Before the catalytic test, the samples were sulfided in a flow of a mixture of H_2/H_2S (15 vol% H_2S) at 673 K for 4 h. Thiophene hydrodesulfurization was performed in the vapor phase in a fixed bed microreactor at atmospheric pressure (thiophene pressure: 24×10^2 Pa, total flow: 6 liter/h). A catalyst charge of about 0.1 g was employed. Specific activities were determined after 16 h on stream in the pseudo-stationary state at 573 K. In these experimental conditions the total conversion of thiophene was always lower than 10%.

Characterization

X-ray diffractograms were recorded on a Siemens D500 diffractometer using Ni-filtered Cu$K\alpha$ radiation. Chemical analyses were carried out by the atomic emission method. Surface areas and pore radii distributions were measured by nitrogen adsorption.

UV–visible diffuse reflectance spectra were recorded in the wavelength range 200–500 nm with a Perkin–Elmer spectrophotometer using the differential method, the reference being pure ZrO_2 prepared by the molten salt method, or $BaSO_4$.

Transmission electron microscopy studies were performed using a Jeol 100CX microscope (resolving power of 0.3 nm). The solids were ultrasonically dispersed in ethanol and the suspension was collected on carbon-coated copper grids.

XPS studies were performed on a Hewlett-Packard 5950 A spectrometer using monochromatic Al$K\alpha$ radiation. The XPS spectra of Zr 3*d*, Mo 3*d*, S 2*p*, and O 1*s* were recorded and their binding energies (BE) referred to the energy of the Zr $3d_{5/2}$ level at 182.0 eV (C 1*s* = 285.0 eV).

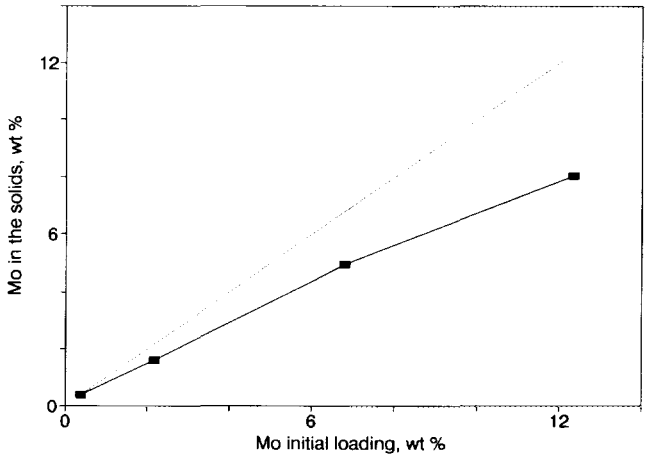

FIG. 1. The amount of Mo (wt%) in the samples as a function of initial loading of Mo in the melts.

RESULTS AND DISCUSSION

1. Characterization of the Solid Oxide Product

1.1. Chemical composition of samples. During molten salt (MS) reactions, yellow precipitates were formed in the melt, a fine pale yellow powder being obtained after water extraction, washing, and drying. The following elements were found in the samples by chemical analyses: Mo (0.5–12.5 wt%), Zr (55–70 wt%), O (around 30 wt%), Na, K, N, and Cl. The last four elements were present as traces (less than 200 ppm). Thus, the solids were mainly composed of Zr, Mo, and O.

The amount of molybdenum found in the samples (calculated as wt% of Mo) versus the initial loading is presented in Fig. 1. Only a part of the initial molybdenum was found in the solid products. With an increase in the initial molybdenum, the proportion in the solid decreased progressively. Since no sublimation of molybdenum products was observed in the course of molten salt reaction, we can conclude that during the reaction some molybdenum was transformed into water soluble compounds (alkali molybdates and dimolybdates). In fact, the amount of molybdenum found in the washing solution was exactly that necessary to fulfill the material balance.

1.2. Phase composition. No reflections from molybdenum-containing phases were detected in the XRD patterns of the samples (molybdenum content varying between 0.3 and 8 wt%). Only the lines of tetragonal (T) and monoclinic (M) zirconia were present (Fig. 2). The relative amount of the T-form increased with the molybdenum content in the samples. Line broadening analysis gave the size of zirconia crystallites as around 10 nm.

From the combined XRD and chemical analysis data, it is clear that samples prepared in the melt may contain

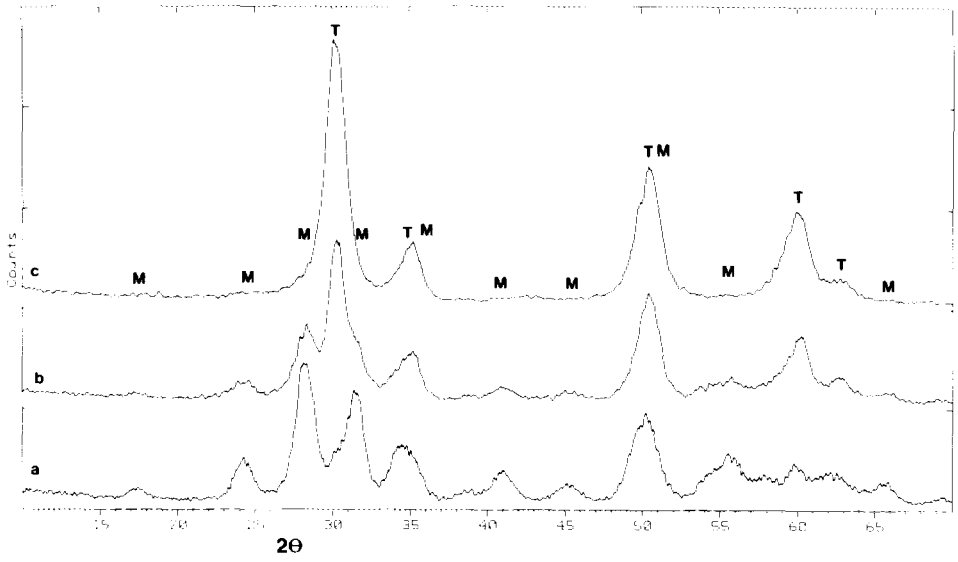

FIG. 2. XRD patterns of the samples with different wt% Mo: 0.6 (a); 2.0 (b); 8.0 (c). T represents tetragonal zirconia; M, monoclinic zirconia.

a large amount of molybdenum in an oxide form, but it does not form any crystalline phases, whatever the initial molybdenum loading.

1.3. UV spectra. To identify the nature of molybdenum species, UV–visible spectra of the samples were obtained under ambient conditions (Fig. 3). Since Mo(VI) has a d^0 electronic configuration, the only absorption band observed was due to the ligand–metal charge transfer transition (LMCT): $O^{2-} \rightarrow Mo^{6+}$, expected in the range 200–400 nm. The width and maximum of this band depended on the molybdenum loading in the samples. To analyze UV–visible spectra semiquantitatively, they were represented as superpositions of two components with asymmetric sigmoidal profiles, using the PEAKFIT (Jandel Corp) program, results being presented in Table 1. The first component, at about 260 nm, corresponds to low-polymerized molybdate species with tetrahedral coordination of Mo atoms (MoO_4^{2-}, $Mo_2O_7^{2-}$). The second, at 300–350 nm is characteristic for polymolybdate with octahedral coordination of Mo (heptamolybdate, octamolybdate). With the increase of Mo loading, continuous growth of absorbance was observed. At the same time, the shape of the spectra changed in favor of the higher wavelength band. Redistribution of the relative intensities of the components also occurred with the increase of Mo content due to the gradual polymerization of the oxospec-

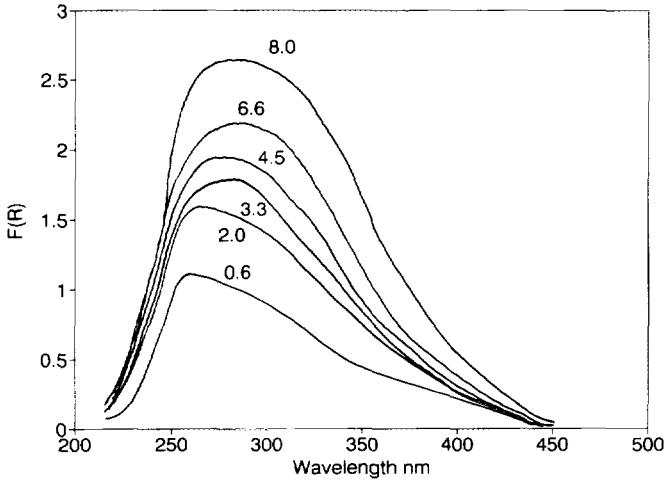

FIG. 3. UV–visible spectra of the samples under ambient conditions. Mo content is indicated by numbers, as wt% Mo.

TABLE 1

Results of the Fitting of UV–Vis Spectra by the PEAKFIT Program

wt% Mo	$F(R)$	Center (nm)	Width (nm)	Area (%)
0.6	0.9	255	73	75
	0.27	342	96	25
2.0	1.57	262	78	70
	0.59	343	81	30
4.5	2.01	260	80	56
	0.88	309	92	44
8	1.56	250	73	33
	1.66	306	84	67

Note. Spectra are presented as superpositions of asymmetric double sigmoidal profiles. Confidence interval 95%; correlation better than 0.999. $F(R)$: Kubelka–Munk function.

ies (see Table 1). This type of behavior as a function loading is common for supported systems and has been observed earlier for the molybdenum species on alumina (26).

1.4. Genesis of the supported systems. Consideration of the mechanism of the molten salt chemistry may explain the genesis of this supported phase. Currently, the chemistry of most elements in molten nitrates is moderately well understood, with many Lux-Flood acid–base reactions (27). The final products of acid-base reactions can be considered to be formed via transfer of the oxide anion:

$$NO_3^- + \text{Acid} = NO_2^+ + \text{Acid} \cdot O^{2-}. \quad [1]$$

For example, acidic zirconium (IV) salts are known to abstract oxygen anions from nitrate anions, to give zirconium oxide (28) according to Eq. [2]:

$$ZrOCl_2 \cdot 8H_2O + 2NO_3^- \rightarrow ZrO_2 + 2\,NO_2 + 2Cl^- + \tfrac{1}{2}O_2 + 8H_2O. \quad [2]$$

Similarly, molybdenum compounds undergo stepwise reactions (eq. [3]–[6]) leading to alkali metal molybdates A_2MoO_4(A = K, Na) (29).

$$(NH_4)_6Mo_7O_{24} \cdot 4H_2O \rightarrow 6NH_3 + 7MoO_3 + 7H_2O \quad [3]$$

$$3MoO_3 + 2NO_3^- \rightarrow Mo_3O_{10}^{2-} + 2NO_2 + \tfrac{1}{2}O_2 \quad [4]$$

$$2Mo_3O_{10}^{2-} + 2NO_3^- \rightarrow 3Mo_2O_7^{2-} + 2NO_2 + \tfrac{1}{2}O_2 \quad [5]$$

$$Mo_2O_7^{2-} + 2NO_3^- \rightarrow 2MoO_4^{2-} + 2NO_2 + \tfrac{1}{2}O_2 \quad [6]$$

With the simultaneous reaction of both Zr and Mo salts in molten nitrates, surface interactions between the growing particles of ZrO_2 and the molybdate anions occur (24). As in aqueous chemistry, mono- or polymolybdate species can be grafted at the surface of the solid since molybdate can polymerize on growing zirconia nuclei. Such polymolybdate species slow down the growth of nuclei in the areas of their grafting, because they remain on the surface of the solid product. Both MoO_3 and $Zr(MoO_4)$ are unstable and react in the molten nitrate. Hence the presence of these phases in the solid products of MS reaction is excluded by the nature of the preparation method.

1.5. Textural properties. Admixture of heptamolybdate in the zirconia considerably increased the specific surface areas of solids obtained, as compared with those of pure or yttria-stabilized zirconia prepared in molten nitrate baths under similar conditions (15), or with zirconias prepared using conventional aqueous methods (the latter are in the range of 100 m^2/g). With molybdate-zirconias, surface areas as high as 220 m^2/g can be obtained, and the specific surface area shows a maximum for samples with 4.5–5.3 wt%. of Mo. Surface areas of noncalcined samples are presented in Fig. 4.

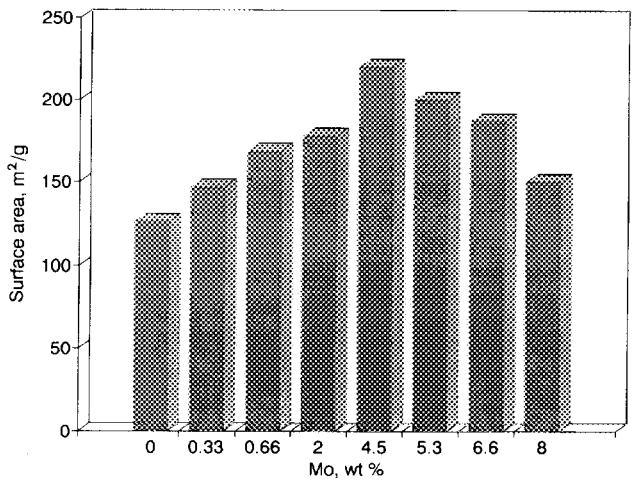

FIG. 4. Specific surface area of noncalcined samples vs Mo loading.

Since the solids were prepared at 773 K in the melt, calcination in air below 773 K does not change their surface areas. To evaluate the thermal stability of the solids, two calcination temperatures (873 and 1073 K) were chosen. Surface areas obtained after calcination are presented in Table 2. It can be seen that 4.5 wt% Mo is optimum not only for the initial value of specific surface, but also for its stability to calcination. Higher or lower Mo loadings lead to lower surface areas after calcination at 1073 K.

Apart from the specific surface areas, the presence of Mo decreased the average size of pores. The pore sizes was around 2 nm in noncalcined and calcined at 873 K samples (Fig. 5a) which is lower than that for pure zirconia prepared in the same conditions (3 nm, Fig. 5b). Calcina-

TABLE 2

Specific Surface Area ($m^2\ g^{-1}$) of Molybdena–Zirconia Samples after Calcination in Air

	Calcination temperature (K)		
Mo (wt%)	Not calcined	873	1073
0	126	70	9
0.6	169	122	7.5
2.0	178	143	34
4.5	220	157	68
8.0	150	126	4.5

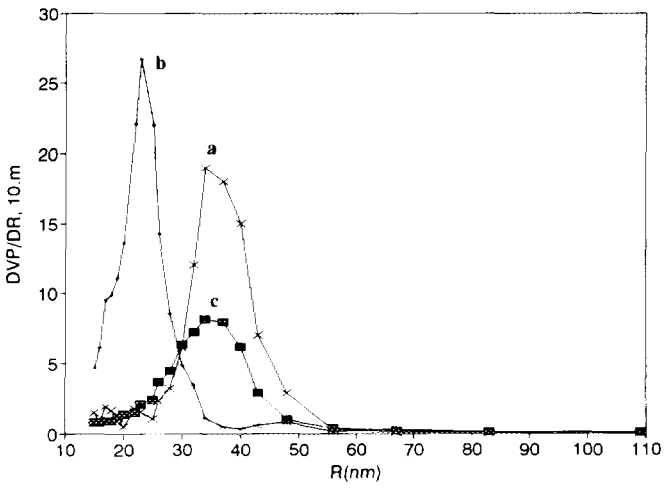

FIG. 5. Distribution of pore radii in pure ZrO_2 prepared in molten nitrate (a); Mo–Zr sample with 4.5 wt% Mo (b); and sample (b) calcined at 1073 K for 2 h (c).

tion at 1073 K led to an increase of average pore radii to 3.5 nm (Fig. 5c).

For all the samples, calcination at 873 K yielded only a slight redistribution of zirconia in favor of the monoclinic form. With a calcination temperature of 1073 K, two situations occurred:

(i) when surface area decreased, well-crystalline M–ZrO_2 (baddeleite, JCPDS Card 37-1484) was formed. This happened for both low-loaded (0.33, 0.66, and 2 wt% of Mo) or high-loaded (equal to or more than 8 wt%) samples, the latter also showing traces of the $Zr(MoO_4)_2$ phase (JCPDS Card 38-1466).

(ii) Samples with intermediate Mo contents (4.5, 5.3, and 6.6 wt% of Mo) were the most stable and retained T-zirconia as the main phase, even after calcination at 1073 K.

DTA-TG analysis has shown (25) that doping of molten reaction mixture by oxoanions such as pyrosulfate or heptamolybdate changes the morphology of samples, increasing their specific surface area and stabilizing the T-variety of zirconia. Oxoanions also improve stability to calcination in air. The work further suggested that, on the basis of TGA data, oxoanions are included in an amorphous Mo-containing phase which is spread over the crystallites of zirconia. This amorphous phase causes stabilization of the T-form of ZrO_2 and provides a high surface area solid and the stabilizing effect persists until the temperature of crystallization of the amorphous phase. In other terms, sintering of the sample requires decomposition of a nonstoichiometric surface compound including Zr and Mo. When the calcination temperature exceeds a critical value, the surface compound decomposes and rapid sintering of the sample occurs.

Here we observe a dependence of the stabilizing effect on the oxoanion (polymolybdate) content. If the latter is too low, sintering of the sample proceeds almost as for pure zirconia, since only a small part of zirconia crystallites is covered by the amorphous material. By contrast, if there is too much Mo in the sample, the amorphous phase itself sinters relatively easily, leading to sublimation of MoO_3, crystallization of M-zirconia and trace amounts of Zr molybdate.

Apparently, intermediate Mo loadings provide an optimum ratio between ZrO_2 crystallites and amorphous matter, so that a morphology consisting of small particles of T-ZrO_2 embedded in the amorphous phase can persist at calcination temperatures as high as 1073 K. Although calcination of the 4.5 wt% Mo sample at 1073 K is accompanied by loss of about $\frac{2}{3}$ of the initial surface area, this value remains 7 times higher than that of a nondoped sample.

In the molten salt preparations, the chemical form of Mo is that of a surface polymolybdate, thus somewhat resembling that in systems prepared by impregnation or other methods, such as the grafting or decomposition of organometallic precursors (30) or by the solid/solid wetting method (31–33). However, for all the preparative methods reported earlier, the specific surface area of the supported molybdenum catalyst was equal to or lower than that of a pure support. Usually, upon an increase of Mo loading, surface area decreases because of the plugging of support pores by the supported material. By contrast, in the case of the molten salt (MS) preparation, the surface area of Mo-containing samples increases with increase of the Mo content. Mo species induce a positive influence on the textural properties of the solids.

2. *Properties of the Solids in the Sulfided State*

X-ray photoelectron spectroscopy was performed on the samples containing 4.5 wt% of Mo in both the oxide and the sulfided states. The binding energy (BE) of the Zr $3d_{5/2}$ level (182.0 eV) was employed as a standard. The values of the binding energies for Mo and S and the surface atomic ratios calculated from the integrated peak areas are presented in Table 3. BE values in the oxide state are typical for Mo(VI) and Zr(IV) oxospecies (13). After sulfidation at 400°C, all the surface Mo(VI) transformed to Mo(IV), as usually observed in molybdenum supported catalysts. Surface atomic ratios calculated from XPS data, within the limits of precision, coincided with those from chemical analysis. The similarity of the XPS and chemically determined Mo/Zr ratio indicates a fine dispersion of the Mo species. High S/Mo atomic ratios may be due to the presence of sulfur species on the surface of zirconia.

Mo samples (4.5 wt%) non-calcined or after calcination at 873 and 1073 K, were sulfided and their catalytic activity

TABLE 3

Binding Energies (BE) of Electronic Cores and Surface Atomic Ratios of the Elements for the Oxide and Sulfided States of Mo/ZrO_2 Samples

Sample (Mo/Zr[a])	BE (eV)		Atomic ratio	
	Mo $3d_{5/2}$	S $2p$	Mo/Zr	S/Mo
0.06 (oxide)	232.4	—	0.07	—
0.06 (sulfided)	228.5	161.8	0.05	5.9
0.22 (oxide)	232.5	—	0.21	—
0.22 (sulfided)	228.6	161.7	0.17	2.8

[a] Mo/Zr ratios obtained from chemical analysis.

measured. Since no loss of Mo was observed during the calcination (and/or sulfidation) the Mo loading was maintained. Figure 6 describes the variation of surface area and the catalytic activities of these samples. Upon calcination at 1073 K, the surface area of the oxide sample decreased from 220 to 68 m^2/g. At the same time, the activity after sulfidation remained constant. Because of sintering, the Mo loading rose from 1.34 to 4.9 atom/nm^2 with calcination. Since catalytic activities remain equivalent, it should be emphasized that calcination and subsequent sulfidation provide the same dispersion of the active phase. This result suggests that a high concentration of Mo can be achieved on such samples and consequently that a large part of the surface area remains unoccupied by molybdate species. The loss in surface area without change in activity suggests that only the fraction of zirconia uncovered by Mo undergoes sintering. These catalysts can be seen as a zirconia surface pimpled with bound

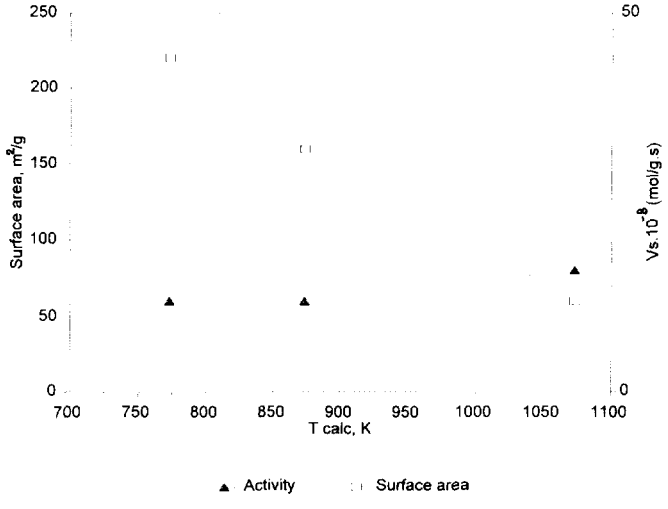

FIG. 6. Specific surface area of Mo–Zr sample (4.5 wt% Mo) and catalytic activity in HDS of thiopene, versus temperatures of calcination.

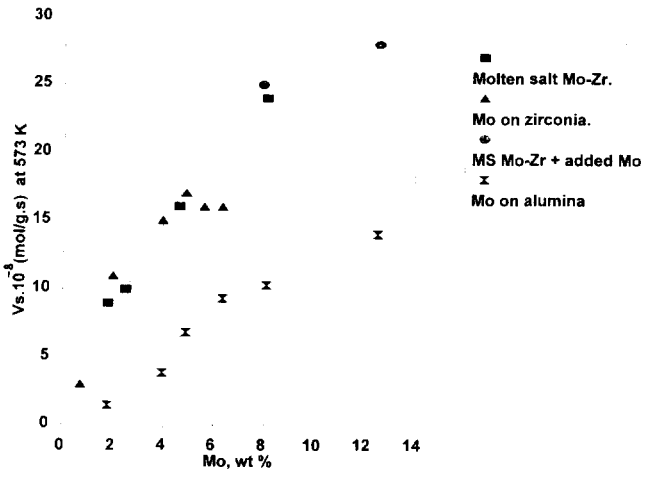

FIG. 7. Catalytic activity of sulfided samples prepared in different ways.

polyanions. During sulfidation, phase transformation and cluster growth occurs to form islands of layered molybdenum disulfide.

In conventional preparation methods, the adsorption of heptamolybdate on alumina (34) or other oxide surfaces (35) involves surface hydroxyl groups in the process of binding oxoanions to the oxide surface. Since molten nitrates are nonaqueous solvents, hydroxyl groups do not exist and interaction between zirconia and the molybdate may occur via nitrate surface ligands. However, after molten salt reaction, upon washing or even simple exposition in air, the samples could be rehydrated, and rehydroxylated, under ambient conditions, due to the dissociative adsorption of water leading to the creation of OH groups. Consequently, for a sample with 4.5 wt% of Mo, a large part of the surface area of zirconia is still available for anchoring additional molybdate species in the classical way. In order to support this assumption, we added Mo by a conventional method to those Mo–Zr catalysts which manifested the highest surface area. The effect of this loading on the catalytic activity is presented in Fig. 7, where Vs represents the specific activity. For comparison, the previous results obtained by Hamon *et al.* (36) and the activity of a reference Mo/Al_2O_3 catalyst are also indicated on Fig. 7. The plateau effect usually observed on supported Mo systems, starting respectively at 7 Mo wt% for ZrO_2 (14, 23) and at 10 Mo wt% for alumina (14, 37), is pushed to a higher limit, of around 12.5 wt%, in the case of the Mo/Mo–Zr catalyst. The MS method also provides samples with loadings as high as 12 wt% of Mo but a loss of Mo is inherent to the preparation method). Interestingly, the two samples (MS and MS + Mo) with similar loadings have the same catalytic activity (see Fig. 7).

TABLE 4

Average Values of Length (L) and Number of Layers of MoS_2 Fringes (N) in Sulfided Samples

	Mo loading (atom/nm^2)	N	L (nm)
Mo–Zr	1.31	1.7	2.9
Mo–Zr + Mo	3.55	2.1	3.0
Mo/Y–Zr	1.4	1.4	2.7
	4.2	1.8	4.5

Note. Comparison with data obtained for Mo deposited on yttria-doped zirconia (31).

The intrinsic HDS activity of Mo/ZrO_2 catalysts was previously found to be twice that of conventional catalysts (14–16) but the low value of the surface area of the zirconia is a handicap. In our case, the preparation method can achieve surface areas comparable to those of alumina; as a consequence, a drastic increase of specific activity per gram of catalyst was obtained.

XPS characterization performed on the highly loaded samples (MS + impregnated Mo: 12.5 wt%) in both calcined and sulfided states, indicates that even at relatively high loading, the fine dispersion remains. Sulfided catalysts with 4.5 and 12.5 Mo wt% loadings were characterized by high resolution electron microscopy (HREM). The supported MoS_2 phase appeared as small crystallites typical of the lamellar structure of molybdenum disulfide. Measurements of the number (N) and the length of fringes (L) on a large number of crystallites allowed the calculation of an average size for the crystallites. Table 4 summarizes the data obtained for 4.5 and 12.5 wt% of Mo loadings. Comparison between these catalysts indicates that length and number of layers are not influenced by the addition of Mo in a conventional way. Only a slight increase in stacking is visible. This suggests that the dispersion remains since the anchoring of extra molybdenum happens on the free surface through a different mechanism. In the case of conventional impregnation methods, and after sulfidation, increasing the Mo loading induced an increase of the average length and number of layers (23). A relationship between EM data and catalytic activity can be suggested, since samples with similar length number of layers prepared by the different methods give similar catalytic activities, indicating that the same dispersion is obtained.

CONCLUSION

As concluding remarks, we can outline several points which seem to be unique advantages of MS method:

— All the other preparation techniques mentioned above imply that support oxide (alumina, zirconia) with desirable properties is prepared beforehand. The MS method provides a one-stage synthesis of the supported oxide system. In this respect, it has a common feature with the sol–gel method.

— The results of MS synthesis are perfectly reproducible. The properties of supported systems, prepared using commercial supports, depend drastically on the properties of the latter (isoelectric point, specific surface, etc.), whereas the properties of the products of MS synthesis are determined by the chemical composition of the reaction mixture and by the conditions of synthesis. At the same time, the MS method appears to be much less sensitive to the details of operational procedure than the coprecipitation and sol–gel techniques. If the composition of a reaction mixture is given, the only parameter strongly influencing the properties of the product is the temperature of the melt. This parameter was previously used to modify the porosity of a stabilized yttrium–zirconia (15). We can expect precise control of the texture can be achieved in this way.

— By its nature, the MS method excludes the possibility of bulk Mo(VI) oxide in the solid product (because the latter reacts easily with the melt). Thus, for high Mo loading, excess Mo, which cannot be accommodated by the oxide surface, transforms to water-soluble molybdate.

— The MS method is essentially a non-aqueous one. Thus in some cases it provides quite a different chemistry of supported species than the conventional techniques. For example, dimolybdate species, which are unstable in aqueous medium, were observed in the molten nitrate bath, and sodium dimolybdate was isolated as a reaction product at high Mo loadings (24).

Although stabilization of high surface area tetragonal zirconia by Mo(VI) species was reported earlier for impregnated catalysts (38), we believe that the unusual features of the MS technique make it useful for the preparation of catalysts. The potential of new solids in the hydrotreating reaction has been shown in this work. Mixed systems (NiMo, CoMo) supported on zirconia prepared from molten salts also demonstrate interesting properties (39). It is likely that opportunities exist for catalytic oxidation using these solids. Furthermore, the MS method can be generalized for preparation of a wide variety of simple or mixed oxide systems deposited on zirconia (40, 41). The many possible uses for these novel solids are evident and their potential is by no means exhausted by those briefly examined so far.

REFERENCES

1. Wash, I. E., Deo, G., Kim, D. S., Vuurman, M. A., and Hu, H., "Proc. 10th Int. Congr. Catalysis, Budapest 1992" (L. Guczi, F.

Solymosi and P. Tétényi, Eds.), Part A, p. 543, Elsevier, Amsterdam, 1993.
2. Hucknall, D. J., "Selective Oxidation of Hydrocarbons," Academic Press, London, 1977.
3. Martin, C., Martin, I., and Rives, V., *J. Chem. Soc. Faraday Trans.* **89,** 4131 (1993).
4. Ono, T., Anpo, M., and Kubokawa, Y., *J. Phys. Chem.* **90,** 4780 (1986).
5. Prins R., de Beer V. H. J., and Somorjai, G. A., *Catal. Rev.-Sci. Eng.* **31,** 1 (1989).
6. Ratnasamy, P., and Sivasanker, S., *Catal. Rev.-Sci. Eng.* **22,** 401 (1980).
7. Massoth, F. E., *Adv. Catal.* **27,** 265 (1978).
8. Ng, K. Y. S., and Guilari, E., *J. Catal.* **92,** 340 (1985).
9. Jin, Y. S., Auroux, A., and Védrine, J. C., *J. Chem. Soc. Faraday Trans.* **83,** 4179 (1989).
10. Miyata, H., Tokuda, S., Ono, T., Ohno, T., and Hatayama, F., *J. Chem. Soc. Faraday Trans.* **86,** 2291 (1990).
11. Ono, T., Miyata, H., and Kubokawa, Y., *J. Chem. Soc. Faraday Trans.* **83,** 1761 (1987).
12. Miyata, H., Tokuda, S., Ono, T., Ohno, T., and Hatayama, F., *J. Chem. Soc. Faraday Trans.* **86,** 3659 (1990).
13. Payen, E., Gengembre, L., Mauge, F., Duchet, J. C., and Lavalley, J. C., *Catal. Today* **10,** 521 (1991).
14. Pratt, K. C., Sanders, J. V., and Christov, V., *J. Catal.* **124,** 416 (1990).
15. Hamon, D., Vrinat, M., Breysse, M., Durand, B., Jebrouni, M., Roubin, M., Magnoux, P., and Des Courières, T., *Catal. Today* **10,** 613 (1991).
16. Duchet, J. C., Tilliette, M. J., Cornet, D., Vivier, L., Perot, G., Bekakra, L., Moreau, C., and Szabo, G., *Catal. Today* **10,** 579 (1991).
17. Portefaix, J. L., Cattenot, M., Dalmon, J. A., and Mauchaussé, C., *in* "Advances in Hydrotreating Catalysis" (M. L. Occelli and R. G. Anthony, Eds), p. 243. Elsevier, Amsterdam, 1989.
18. Tanabe, K., *Mat. Chem. Phys.* **13,** 347 (1985).
19. Srinivasan, R., Hubbard, C. R., Cavin, O. B., and Davis, B. H., *Chem. Mater.* **5,** 27 (1993).
20. Mercera, P. D. L., van Ommen, J. G., Doesburg, E. B. M., Burggraaf, A. J., and Ross, J. R. H., *Appl. Catal.* **57,** 127 (1990).
21. Duchet J. C., Tilliette M. J., and Cornet D., *Catal. Today* **10,** 507 (1991).
22. Durand, B., Ceramic Powders, p. 413. Elsevier, Amsterdam, 1983.
23. Vrinat, M., Hamon, D., Breysse, M., Durand, B., des Courieres, T., *Catal. Today* **20,** 273 (1994).
24. Afanasiev, P., Geantet, C., and Kerridge, D. H., *J. Mater. Chem.* in press (1995).
25. Afanasiev, P., Geantet, C., and Breysse, M., *J. Mater. Chem.* **4,** 1653 (1994).
26. Jeziorowski, H., and Knözinger, H., *J. Phys. Chem.* **83,** 1166 (1979).
27. Kerridge, D. H., *in* "Chemistry of Non-aqueous Solvents" (J. J. Lagovski, Ed.), Part B, Vol. V, p. 270, Academic Press, New York, 1978.
28. Kerridge, D. H., and Cancela Rey, J., *J. Inorg. Nucl. Chem.* **39,** 405 (1977).
29. Habbouch, D. A., and Kerridge, D. H. *Thermochim. Acta* **10,** 187 (1974).
30. Startsev, A. N., Klimov, O. V., and Khomyakova, E. A., *J. Catal.* **139,** 134 (1993).
31. Del Arco, M., Carrazan, S. R. G., Rives, V., Gil-Llambias, F. G., and Malet, P., *J. Catal.* **141,** 48 (1993).
32. Leyrer, J., Zaki, M. J., and Knözinger, H., *J. Phys. Chem.* **90,** 4775 (1986).
33. Xie Y. C., and Tang, Y. Q., *in* "Advances in Catalysis" (D. D. Eley, H. Pines, P. B. Weisz, Eds.) Vol. 37, p. 1, Academic Press, New York, 1990.
34. Wang, L., and Hall, K., *J. Catal.* **77,** 232 (1982).
35. van Veen, J. A. R., and Hendriks, P. A. J., *Polyhedron* **5,** 75 (1986).
36. Hamon, D., Vrinat, M., Breysse, M., Durand, B., Beauchesne, F., and des Courières, T., *Bull Soc. Chim. Belg.* **100**(11–12), 933 (1991).
37. de Beer, V. H. J., van der Aalst, M. J. M., Machiels, C. J., and Schuit, G. C. A., *J. Catal.* **43,** 78 (1976).
38. Valigi, M., and Gazzoli, D., in "Proc. 10th Intern. Symp. Reactivity of Solids," Dijon, August 27–31, 1984. (P. Barret, L. C. Dufour, Eds.), p. 91, Elsevier, Amsterdam, 1985.
39. Afanasiev, P., Geantet, C., Breysse, M., and des Courières, T., "ACS Meeting, Washington DC, August 21–26, 1994," *ACS Preprints Symp.* **39,** 598, 1994.
40. Afanasiev, P., Geantet, C., and Breysse, M., "Int. Symp. on Soft Chemistry Routes to New Materials, 6–10 September 1993, Nantes, France," p. 111.
41. Geantet, C., Afanasiev, P., Breysse, M., and des Courières, T., *in* "Proceedings, 6th Int. Symp. on the Scientific Bases for the Preparation of Heterogeneous Catalysts, Louvain-la-Neuve 1994" Book of Abstracts Vol. 1, p. 273.